Fluorescence-line narrowing in CdSe quantum dots: Surface localization of the photogenerated exciton

M. Nirmal, C. B. Murray, and M. G. Bawendi
Department of Chemistry, Massachusetts Institute of Technology, 77 Massachusetts Avenue, Cambridge, Massachusetts 02139
(Received 27 December 1993)

The electronic properties of shallow band-edge surface traps in nanometer-size CdSe quantum dots are probed using fluorescence-line-narrowing spectroscopy. We find large changes in electron-hole-pair radiative lifetimes and couplings to LO phonons as the temperature is changed from 1.75 to 10 K. We attribute these changes to the localization of the photogenerated hole at the surface of the dots, accompanied by thermally activated motion between these surface localized states. A simple model based on the observed exciton–LO-phonon couplings is constructed to estimate the extent of hole localization in the luminescing state. A size-dependent study (20–80 Å diameter) indicates that surface effects diminish rapidly with increasing size.

I. INTRODUCTION

Semiconductor nanocrystallites (quantum dots) which are small compared to the bulk exciton radius have unique properties associated with the spatial confinement of the electronic excitations. These crystallites have discrete electronic states, in contrast to the bulk band structure, with an effective band gap blue shifted from that of the bulk.[1] They are also characterized by large surface to volume ratios. A 23-Å-diameter quantum dot of CdSe, for example, has an effective band gap blue shifted by 0.6 eV from the bulk, and has roughly 40% of its ~400 atoms at the surface. Structural probes indicate the presence of a crystalline core while the surface structure still remains largely unresolved.[1,2] Recent theoretical efforts have thus been devoted primarily to the ideal quantum dot with an infinite potential at the interface. Unlike quantum wells and wires which can be grown epitaxially, experimental studies suggest that the surface of nanocrystallites plays a potentially crucial role in their electronic and optical properties.[3–5]

This paper focuses on the luminescence properties of CdSe quantum dots capped with trioctylphosphine chalconide groups. We use fluorescence line narrowing to observe changes in coupling to LO phonons as temperature and dot size are varied. We find that the luminescence spectra display many of the features characteristic of disordered II-VI systems where hole localization is observed.[6,7] We attribute the similarities between the data on quantum dots and that on the disordered systems to the presence of interfacial roughness (surface disorder) in the nanocrystallites. We use a simple model based on the observed changes in LO-phonon coupling to estimate the extent of hole localization in the luminescing state. We find that the effects of disorder diminish rapidly with increasing crystallite diameter.

II. EXPERIMENT

Quantum dots of CdSe were produced from the pyrolysis of dimethylcadmium and tri-*n*-octylphosphine selenide (TOPSe) in a solution of 50% tri-*n*-octylphosphine (TOP) by weight and 50% tri-*n*-octylphosphine oxide (TOPO) using a procedure described elsewhere.[2] The method produces quantum dots of CdSe with the surface Cd atoms passivated with TOPO and TOPSe molecules.[8] The samples prepared for this study ranged in size from 23- to 83-Å diameter with a standard deviation of ~10%. The dots were studied dispersed in the growth medium (TOPO/TOP) at a concentration of ~1.4% volume fraction, avoiding contact with air to prevent surface oxidation of the dots.

Samples were placed in an optical helium vapor flow cryostat to obtain low-temperature luminescence. Temperatures between 1.75 and 2.1 K were attained by immersion in superfluid helium under a regulated vacuum. Temperatures >2.1 K used helium vapor. Nanosecond Nd:YAG/dye (YAG is yttrium aluminum garnet) laser systems (6-nsec pulses) were used as excitation sources. The laser power was attenuated [$\sim 20(\mu J/mm^2)$/pulse] to ensure that the detected luminescence was linear with respect to the excitation intensity. The luminescence was dispersed through a 0.66-m single spectrometer and detected by a time-gated optical multichannel analyzer (OMA) to obtain spectra. Emission decays were recorded using a 500-MHz digitizing oscilloscope, a photomultiplier tube (2-nsec resolution), and a 0.75-m subtractive double spectrometer in order to eliminate scattered laser light.

III. OBSERVATIONS AND ANALYSIS

The broad spectral features observed in the absorption spectrum [Fig. 1(a)] of samples of CdSe quantum dots are indicative of sample inhomogeneities.[1–3,9–11] Excitation to the blue of the first absorption maximum yields band-edge emission from the entire size distribution [~65-meV full width at half-maximum (FWHM)] [Fig. 1(a)]. However, as in many inhomogeneously broadened systems, selective excitation of a class of quantum dots results in fluorescence line narrowing (FLN).[3] Information from a single class of crystallites (i.e., those particles

0163-1829/94/50(4)/2293(8)/$06.00

that because of size, defects, surface structure, environment, etc. absorb at the same energy) can be obtained by exciting on the red edge of the first absorption feature and selectively exciting the largest crystallites. The FLN spectrum then shows a well-resolved LO-phonon progression with a spacing of ~25 meV corresponding to the bulk LO-phonon frequency [Figs. 1(a) and 1(b)]. The shape of the FLN spectrum is nearly insensitive to the excitation energy as long as it is on the red side of the absorption peak, where size selection is possible as explained in Ref. 3. The zero LO-phonon linewidth in the FLN spectrum is a measure of the homogeneous linewidth and ranges from ~4 to ~17 meV, with the largest particles (80-Å diameter) having the narrowest linewidth.[12]

The exciton–LO-phonon coupling strength (the Huang-Rhys parameter S) is related to the integrated intensity ratios of the one-phonon line (1PL) to the zero-phonon line (ZPL). The LO mode has the Cd and Se atoms vibrating out of phase within each unit cell. Since the Cd-Se bond is relatively polar, the LO mode interacts with charge distributions within the crystallite through the Fröhlich interaction.[13–16] Coupling to lattice vibrations is then expected to increase with localization of a carrier at the surface of the crystallite. Conversely, the observed coupling strength can in principle be used to infer the localization of charge within a crystallite.[17,18]

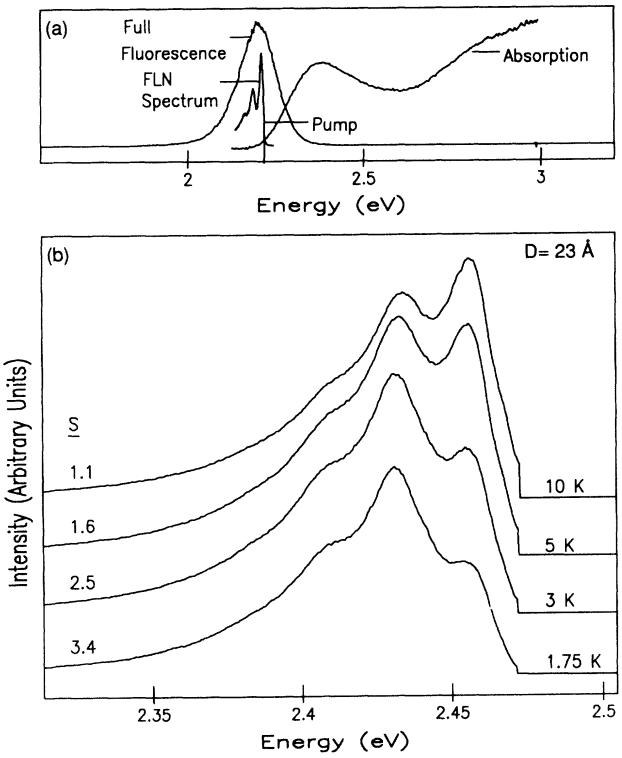

FIG. 1. (a) Broad inhomogeneous sample absorption and luminescence spectra compared with the fluorescence line narrowed emission (FLN spectrum) for ~30-Å dots at 10 K. The large decrease in linewidths in the FLN spectrum allows observation of LO-phonon structure. The shift between absorption and luminescence in the inhomogeneous spectra is strongly dependent on the size distribution and is not a "single-particle" property. (b) Temperature dependence of the LO-phonon structure in the fluorescence line narrowed spectrum of 23-Å dots. The extracted coupling constant S is given for each spectrum. The intensities are normalized for ease in comparison. The sharp cutoff in the blue (~2.47 meV) is an artifact of the data collection.

A. Temperature-dependent LO-phonon coupling

Figure 1(b) shows that the shape of the FLN spectrum of 23-Å diameter CdSe quantum dots changes dramatically between 1.75 and 10 K. Previous studies have proposed that the long-lived (μs) band-edge emission originates from the recombination of surface-localized holes and delocalized electrons.[3] Surface-localized holes are expected to have much larger effective masses than delocalized ones,[19] so that the kinetic energy of the hole is not increased substantially upon localization, as might be expected from bulk arguments. These surface states can thus in principle lead to strong localization with only a small change in energy. We suggest here as a model for the analysis that the electronic potential for the surface trapped hole is randomly corrugated. Such disordered systems contain two kinds of states: localized states in which the probability amplitude decays exponentially from a center of localization, and delocalized or extended plane-wave states.[20] At 1.75 K the hole is trapped in a potential well on the surface, and there is a large separation of charge between the delocalized electron and the trapped hole. The resulting charge imbalance induces a lattice polarization and causes an enhanced coupling to LO phonons which is reflected in the increased ratio of the one to zero-LO-phonon lines in Fig. 1(b). As the temperature is raised, spatial transfer of the hole across the disordered surface is enabled via inelastic processes. The hole migrates from site to site with the energy mismatch between adjacent trap sites being made up by acoustic phonons.[21] The increased overlap between the electron and the thermally delocalized hole decreases the charge imbalance and consequently also the coupling strength. Figure 2 shows the relative change in coupling strength for 33-Å-diameter crystallites as the temperature is increased from 1.75 to 10 K. The quantum yield remains unchanged over this temperature range, so that an increase in the zero-phonon line emission intensity is compensated for by a decrease in the higher phonon satellites.

In a displaced harmonic oscillator model (along the LO vibrational coordinate) the Huang-Rhys parameter S (the coupling strength) is given by the square of the ratio of integrated intensities of the one LO-phonon line to the zero-LO-phonon line. The observed fluorescence spectrum is a convolution of the single-particle or homogeneous fluorescence spectrum, the homogeneous absorption spectrum, and the inhomogeneous size distribution. The single-particle absorption and fluorescence spectra are assumed to have the form

$$A(\nu,\nu')=\sum_{m=0}^{2}\frac{\alpha_a^m}{m!}\exp\left\{-\frac{[\nu-(\nu'+m\omega_{\mathrm{LO}})]^2}{2\gamma_{a,m}^2}\right\}, \qquad (1)$$

$$F(\nu,\nu')=\sum_{m=0}^{2}\frac{\alpha_f^m}{m!}\exp\left\{-\frac{[\nu-(\nu'-m\omega_{\mathrm{LO}}-\Delta)]^2}{2\gamma_{f,m}^2}\right\}, \quad (2)$$

where ν' is the position of the zero-LO-phonon line in absorption, ω_{LO} is the LO-phonon frequency ($\sim$24 meV for 23-Å-diameter quantum dots),[12] Δ is the shift between the peak of the zero-LO-phonon lines in absorption and fluorescence (the Stokes shift), $\alpha_{a(f)}$ is the exciton–LO-phonon coupling constant in absorption (fluorescence), and $\gamma_{a(f)}$ is the linewidth of the phonon replicas. The sums are over the first three LO-phonon replicas which are experimentally cleanly observed. The observed FLN spectrum F_{LN} is given by the convolution

$$F_{\mathrm{LN}}(\nu)=\int A(\nu_{\mathrm{exc}},\nu')F(\nu,\nu')\exp\left\{-\frac{(\nu'-\nu_0)^2}{2\gamma_{\mathrm{inh}}^2}\right\}d\nu', \quad (3)$$

where ν_0 is the center of the Gaussian inhomogeneous distribution, ν_{exc} is the excitation energy, and γ_{inh} is the inhomogeneous linewidth. The Huang-Rhys parameter $S(\alpha_f^2)$ is determined by constructing single-particle absorption [Eq. (1)] and fluorescence [Eq. (2)] spectra, convoluting with the particle distribution as in Eq. (3), and fitting with the experimentally observed FLN spectrum. The extracted values of S were insensitive to the exact value of the coupling strength in absorption (α_a) which were assumed to be between 0.2 and 0.7, consistent with Raman studies.[13,14]

A simple continuum model can be used to extract the charge distribution from the experimentally observed exciton-phonon coupling. In our model the hole is assumed to be localized on the surface in a sphere of radius r_h, while the electron is delocalized over the volume of the crystallite (a sphere of radius R) (Fig. 3, inset). Both the electron and hole are placed in totally symmetric $1S$ particle-in-a-sphere wave functions. The phonons are treated within a continuum model using the LO vibrational eigenmodes of a semiconductor sphere. The charge distribution interacts with the LO modes through the potential[15,16]

$$\Phi_{n,l,m}(r)\propto j_l(k_{n,l}r)Y_l^m(\theta,\phi),$$

where $\Phi_{n,l,m}(r)$ is the potential generated by the LO vibration, $j_l(k_{n,l}r)$ is a spherical Bessel function, $Y_l^m(\theta,\phi)$ are spherical harmonics, and the boundary condition $\Phi_{n,l,m}(R)=0$ determines the values of the $k_{n,l}$. For a particular hole radius r_h, the coupling strength S is given by[15,16]

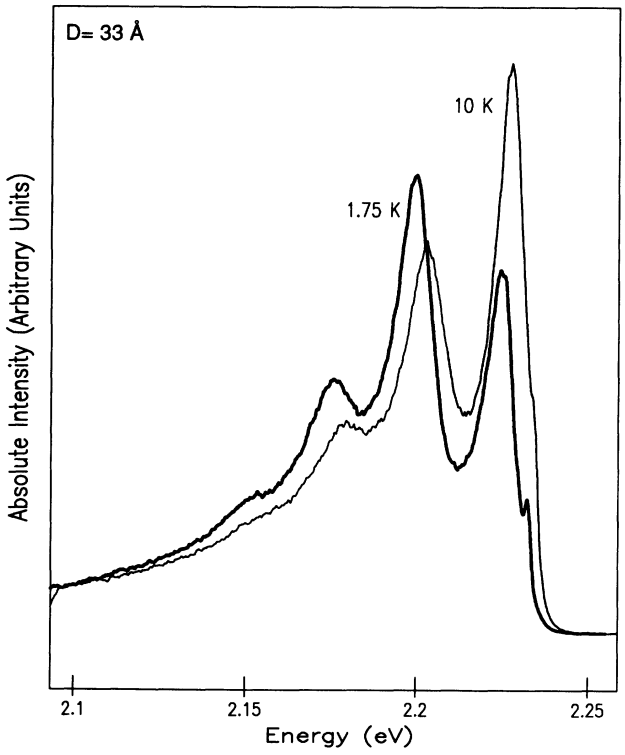

FIG. 2. Fluorescence line narrowed spectrum of 33-Å dots at 1.75 (heavy line) and 10 K (light line). Both the one- to zero-LO-phonon ratio and the Stokes shift increase with decreasing temperature. The small narrow peak in the 1.75-K spectrum and the small shoulder in the 10-K spectrum, both at $\sim$2.23 meV, are due to leftover scattered laser light which we keep for calibration.

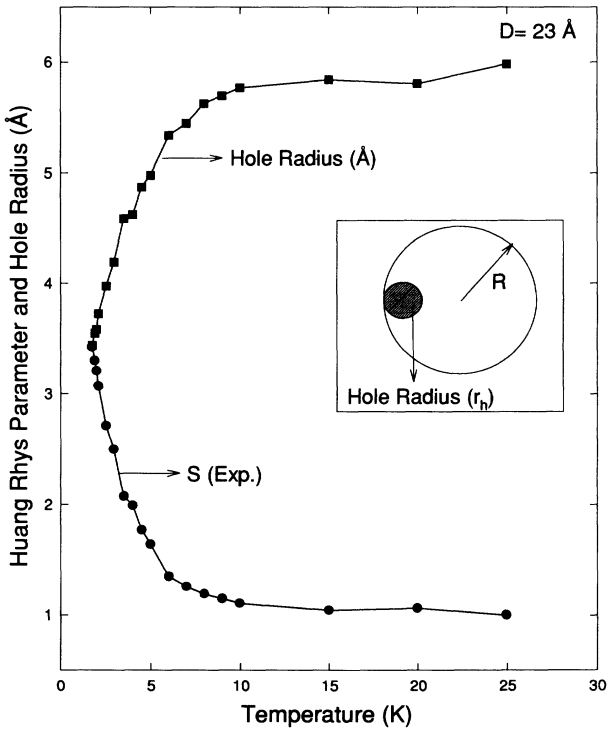

FIG. 3. Temperature-dependent Huang-Rhys parameter (S) extracted from the LO-phonon ratio (circles). The surface-localized hole diameter is calculated from the Huang-Rhys parameter (squares). (Inset) Schematic of the model used for hole localization.

$$S=\sum_{k_{n,l}}\frac{1}{(\hbar\omega_{\mathrm{LO}})^2}|v(n,l,m)|^2 ,$$

where

$$v(n,l,m)=e\int d^3r_e d^3r_h \rho_h(r_h)\rho_e(r_e)$$

$$\times[\Phi_{n,l,m}(r_h)-\Phi_{n,l,m}(r_e)] ,$$

and where $\rho_e(r_e)$ and $\rho_h(r_h)$ are the electron and hole charge densities, respectively.

The hole radius r_h is then used as an adjustable parameter to match experimental and calculated Huang-Rhys parameters S. Figure 3 shows the temperature dependence of the experimentally obtained Huang-Rhys parameter for 23-Å-diameter crystallites and the extracted hole localization radius using $l=0$, $n=1-4$ and $l=1$, $n=1-5$ confined LO modes in the calculation (contributions from higher modes are negligible). The model gives a reasonable value of ~6 Å for the hole radius at 10 K (mostly delocalized), and a significantly smaller hole radius of ~3.5 Å at 1.75 K (mostly localized) with an apparent sharp transition at ~10 K. The observed coupling strength at 1.75 K is an order of magnitude larger than that expected for both the electron and hole delocalized.[16]

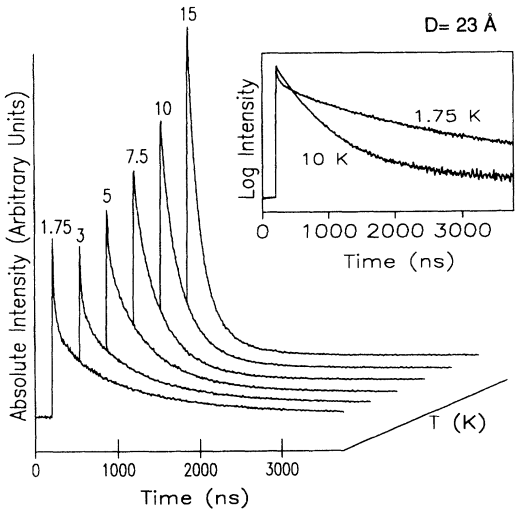

FIG. 4. Temperature-dependence of the luminescence decay for 23-Å-diameter dots from 1.75 to 15 K. The scale on the linear plot is an absolute scale showing the increase in initial radiant intensity with increasing temperature under identical excitation conditions. The apparent higher quantum yield at 1.75 K is from the increased collection efficiency when the sample is immersed in superfluid helium. (Inset) Log of the decays for the lowest and highest temperatures. The decays in the inset are normalized to show clearly the trend from single to multiple exponential character. The initial component speeds up while the tail lengthens.

B. Temperature-dependent lifetimes and Stokes shifts

The temperature dependence of the radiative lifetimes and the Stokes shifts verify the consistency of the model. Radiative recombination times are strongly dependent on overlap of electron and hole wave functions. The temperature-dependent localization is reflected in increased lifetimes with decreasing temperatures. The samples studied luminesce at the band edge with high quantum yield (up to 90% relative to Rhodomine 6G) at the low temperatures of this work. More importantly, the quantum yield Y_Q remains constant over the temperature range studied. The temperature dependence of the quantum yield $Y_Q(T)=\gamma_{\mathrm{rad}}(T)/[\gamma_{\mathrm{rad}}(T)+\gamma_{\mathrm{nr}}(T)]$ comes from both the radiative $\gamma_{\mathrm{rad}}(T)$ and the nonradiative $\gamma_{\mathrm{nr}}(T)$ rates. It is highly unlikely that both these rates have the same temperature dependence. A temperature-independent quantum yield must then imply either that the Y_Q is actually unity in our sample at low temperatures, or more likely that the sample contains two qualitatively different classes of crystallites: A majority of crystallites which luminesce with Y_Q of one and a subset which contain nonradiative recombination centers and are thus dark.[22] In either case, the experimentally observed temperature dependence of the emission lifetimes can be assigned to changes in the radiative recombination rate.

Figure 4 shows the temperature dependence of the luminescence decays for 23-Å-diameter crystallites. These decays are taken at the one-phonon line to completely eliminate laser scattering. Zero-phonon line decays show the same temperature dependence and the same dynamics. At the lowest temperatures the decays are strongly nonexponential with an initially comparatively fast (~10–50 nsec) component followed by a long multiexponential tail (~3 μs). The decays become more uniexponential as the temperature is increased [Fig. 4 (inset)] with a dramatic decrease in the lifetime of the long tail accompanied by an increase in the initial radiant intensity which conserves quantum yield [Fig. 4 (main)].

Optical excitation places the electron and hole in delocalized core states where the kinetic energy of the hole exceeds the surface potential fluctuations. Previously ob-

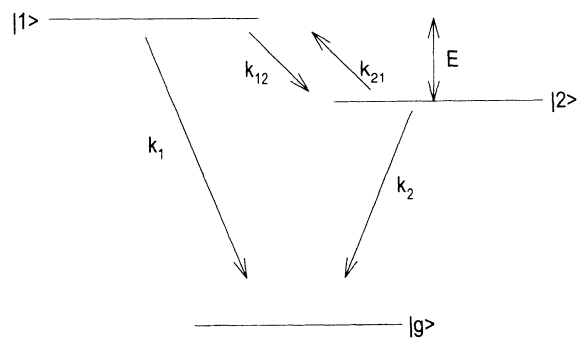

FIG. 5. Three-state model to capture the principal behavior of the relaxation process as explained in the text.

served[3] rapid relaxation ($\sim$100 psec) by acoustic-phonon emission thermalizes the hole, bringing it within the disordered surface band. At the lower temperatures further energy relaxation requires phonon-assisted tunneling between localized surface states. Assuming an exponential tail of localized states,[23] the number of final states declines rapidly as the hole relaxes deeper within the surface band. Since rates for this process depend on the density of final states and interactions between localized states,[24] relaxation by phonon-assisted transitions between localized surface states is considerably slower than relaxation in the delocalized states. Above 10 K, where the LO-phonon coupling suggests that the hole is nearly delocalized, the dynamics become less sensitive to inhomogeneities in the local environment. This may explain the increasing degree of single-exponential character to the decays at the higher temperatures.

The temporal resolution of our experimental setup ($\sim$10 nsec) obscures the initial rapid hole relaxation ($\sim$100 psec) into the localized surface band. Taking this into account, we suggest that the initial relatively fast component ($\sim$10–50 nsec) observed at the lowest temperatures represents hole transfer between surface-localized states. The long multiexponential component ($\sim$3 μs) is then due to a dispersion in radiative lifetimes from the various trap sites on various crystallites.

A complete description of the low-temperature dynamics of electron-hole recombination requires knowledge of the density of localized states and the corresponding exciton–acoustic-phonon couplings with modes of both the crystallites and the matrix in which they are embedded, all of which are poorly understood. A simple three-state model (Fig. 5), however, reproduces the essential physics and features of the observed temperature dependent dynamics. In Fig. 5, $|g\rangle$ is the ground state while $|1\rangle$ and $|2\rangle$ represent surface states with $|1\rangle$ mostly delocalized and $|2\rangle$ deep into the localized band. E is the energy separation between the two upper states, k_1 and k_2 are the corresponding radiative lifetimes, while k_{12} and k_{21} are the transfer rates between the two surface states with k_{21} determined by microscopic reversibility. Figure 6 shows that the temperature dynamics of such a three-state system with $k_1=0.008$ nsec^{-1}, $k_2=0.000\,69$ nsec^{-1}, $k_{12}=1$ nsec^{-1}, $E=0.5$ meV, and with the instrument response (10 nsec) convoluted in, reproduces the essential character of the experimental data (Fig. 4). At higher temperatures the thermal repopulation of $|1\rangle$ is significant, and the observed decay is then dominated by k_1 and appears uniexponential. At lower temperatures, where the thermal repopulation becomes negligible, the decays in Fig. 6 clearly show a fast component corresponding to transfer from $|1\rangle$ to $|2\rangle$, and a long tail dominated by k_2. Consistent with conservation of quantum yield, the initial radiant intensity in Fig. 6 increases with increasing temperature. Comparison of Figs. 4 and 6 shows that a simple three-state model captures the essential physics of the problem.

Radiative recombination rates are proportional to the oscillator strengths or $|\langle\Phi_e|\Phi_h\rangle|^2$, where $\Phi_{e(h)}$ is the electron (hole) envelope function. The model charge distribution of Sec. III A (Fig. 3) gives an order of magni-

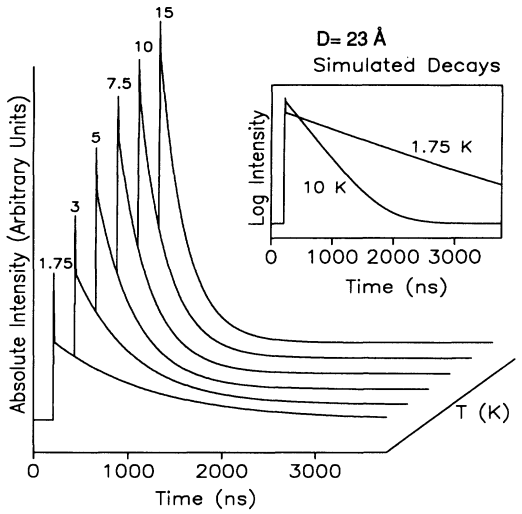

FIG. 6. Simulated temperature-dependent decays from 1.75 to 15 K using the simple three-state model of Fig. 5, and with the $\sim$10-nsec instrument response convoluted in. (Inset) Normalized decays on a log scale as in Fig. 4.

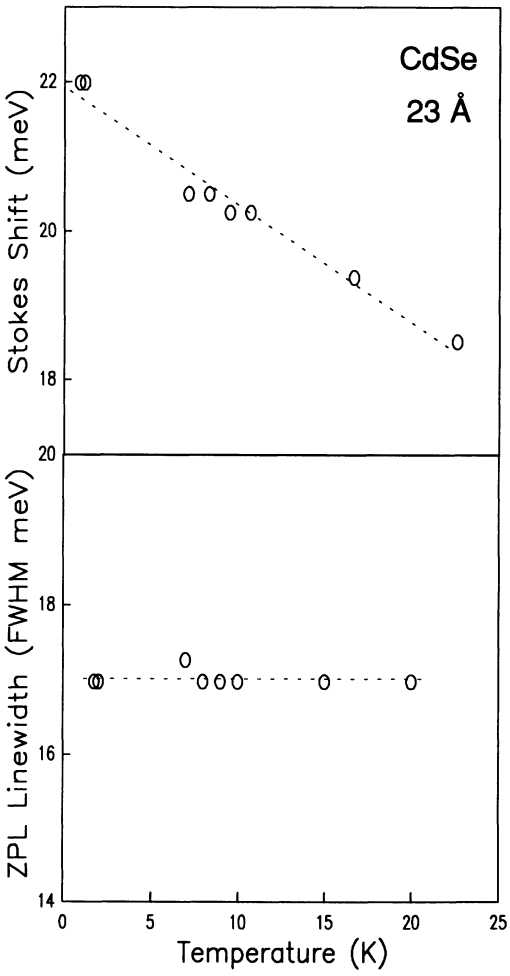

FIG. 7. Comparison of the temperature dependence of the Stokes shift (top) and of the zero LO-phonon (ZPL) linewidth (bottom). The dotted lines are guides to the eye.

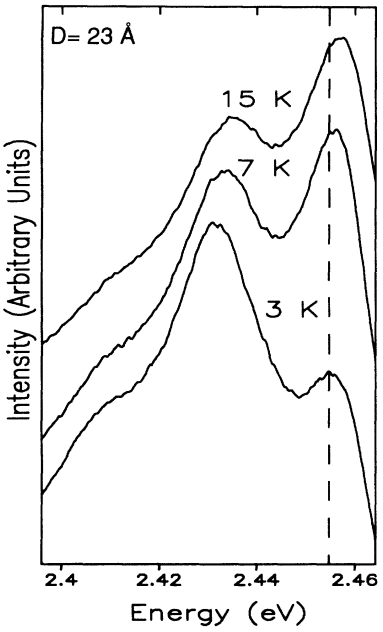

FIG. 8. Temperature-dependent FLN spectra of 23-Å dots at the same excitation energy showing the increase of the Stokes shift with decreasing temperature.

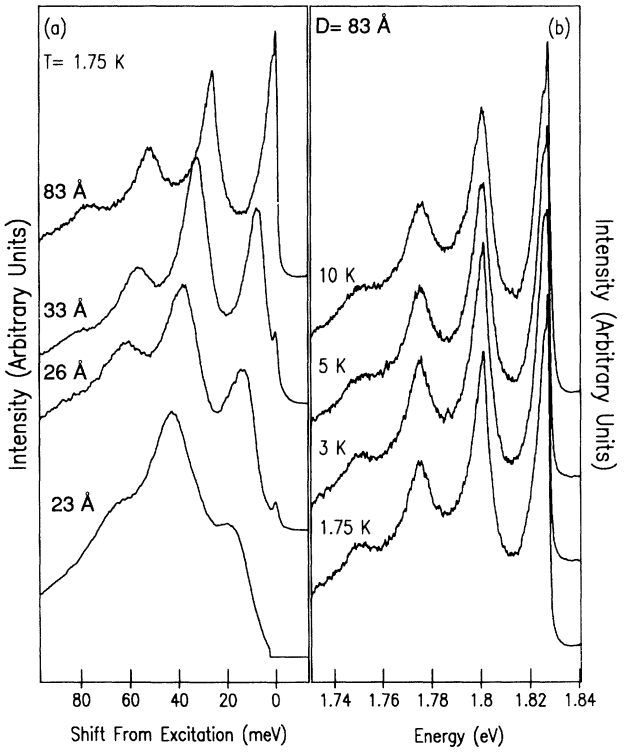

FIG. 9. (a) Size dependence of the FLN spectrum at 1.75 K showing the decrease in LO-phonon coupling with increasing size. The excitation energy was adjusted to account for the red-shift of the absorption with increasing size. The plot is referenced to the laser excitation energy. (b) Lack of temperature dependence of the FLN spectrum for the larger dots (83 Å). The small narrow peak at 0 meV in (a) and at ~1.825 meV near the top of the zero LO-phonon line in (b) is leftover scattered laser light.

tude change in radiative rate from the lowest to the highest temperatures, consistent with the data of Fig. 4 and the modeling of Fig. 6.

The temperature dependence of the Stokes shift is also consistent with thermal activation to higher-lying localized states within the surface band. Figures 7 and 8 shows that the emission spectrum shifts smoothly to the blue with increasing temperature, with the Stokes shift decreasing from ~22 to ~19 meV as the temperature is raised from 1.75 to 15 K. Such behavior has been reported for localized excitons in a wide range of random ternary II-VI alloys.[25] The Stokes shift may result from coupling to acoustic phonons, from relaxation down a purely electronic ladder of (surface) states, or more likely a combination of both. In the acoustic-phonon picture the Stokes shift and the width of the homogeneous line should be correlated. The homogeneous linewidth represents a Frank-Condon profile, and the Stokes shift is accounted for by emission of the acoustic phonons. At the other extreme, the linewidth is explained by the strong coupling of the delocalized core state to the surface electronic states (lifetime broadening) convoluted with the spread in surface energies. Comparison of the Stokes shift and the linewidth (Fig. 7) shows that while the Stokes shift increases down to the lowest temperatures, the linewidth is virtually unchanged between 1.75 and 15 K. The lack of correlation between the Stokes shift and the linewidth strongly implicates an electronic process as a significant contributor to both the Stokes shift and the linewidth. The previous observation that the Stokes shift develops during the first few 100 psec is also consistent with an electronic relaxation from mostly delocalized to mostly localized surface states.

C. Size dependence

The synthesis allows a smooth variation of average crystallite diameter from ~2 to ~10 nm. The smallest crystallites in the series lie in the strong confinement region where the exciton Bohr radius (~56 Å in CdSe) is significantly larger than the crystallite radius. Strong confinement implies that the electron and hole kinetic energies greatly exceed the Coulomb energy between them. The electron and hole are then independently confined. In the intermediate confinement region, where the mean crystallite radius approaches the exciton Bohr radius, the larger effective mass of the hole compared to that of the electron causes the confinement energy of the hole to become comparable to the Coulomb attraction.[26] While the electron remains delocalized, the effect of the Coulomb interaction in principle is to localize the hole toward the center of the crystallite.[27] This effect, combined with the dramatic decrease in surface-to-volume ratio with increasing crystallite diameter, is expected to make surface trapping of the hole less probable toward the intermediate confinement regime.

Figure 9(a) shows that exciton–LO-phonon couplings at 1.75 K, as reflected by the ratio of the one-LO-phonon line to the zero-LO-phonon line, decrease dramatically as the crystallite diameter is increased from 23 to 83 Å. The

homogeneous linewidth in emission (γ_{LO}) and the Stokes shift (Δ) also decrease dramatically with increasing crystallite diameter, from $\gamma_{LO} \sim 17$ meV and $\Delta \sim 18$ meV for the 23-Å-diameter particles to $\gamma_{LO} \sim 4$ meV and $\Delta \sim 1$ meV in the case of the 83-Å-diameter particles. Figure 9(b) shows that there is essentially no temperature dependence to the luminescence spectrum of the largest (83 Å) crystallites from 1.75 to 10 K, consistent with a decrease in the importance of a disordered potential for the hole. Figure 10 shows that the temperature dependence of the change in the Huang-Rhys parameter is strongly size dependent. The largest crystallites show essentially no temperature dependence to S, while the smallest ones show the strong increase in S with decreasing temperature as discussed in Sec. III A. These experimental observations are consistent with a significant decrease in the importance of surface electronic states with increasing crystallite diameter. Figure 11 shows that the luminescence lifetime is also found to dramatically decrease with increasing crystallite diameter, from ~ 3 μs for the 23-Å crystallites to ~ 50 nsec for the 83-Å-diameter ones, with essentially no change in the quantum yield, consistent with a decrease in surface localization of the hole with increasing crystallite size.

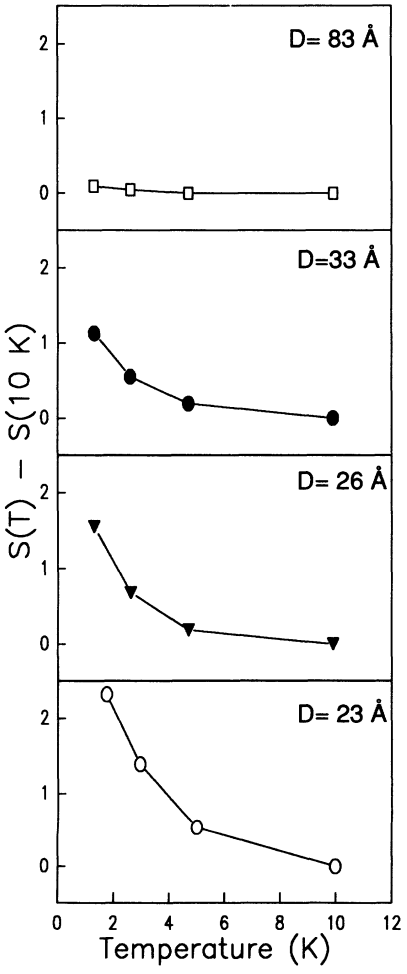

FIG. 10. Size dependence of the temperature-dependent Huang-Rhys parameter.

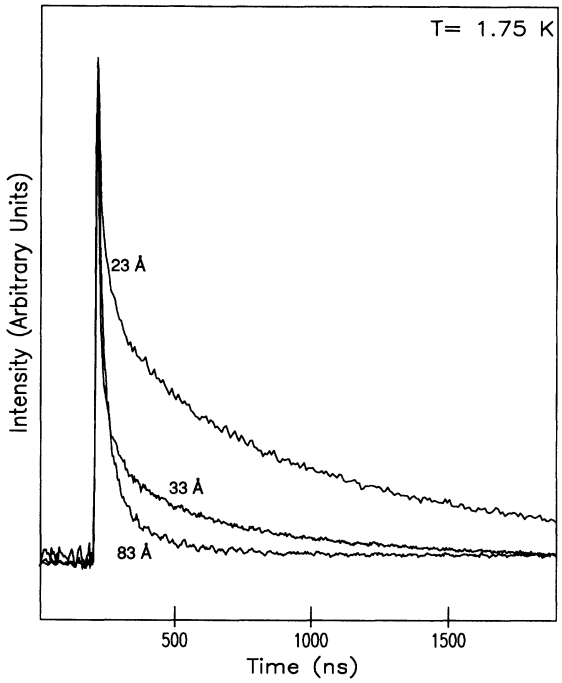

FIG. 11. Size dependence of the luminescence decay at 1.75 K showing the large increase in radiative lifetime with decreasing size. The decays are normalized to the same initial radiant intensity.

The true electronic states of the crystallites must include both surface and core components. Resonances between core and surface states have previously been used to explain the fast (100 psec) dynamics of the band-edge luminescence.[3] The surface-to-volume ratio is then an important factor in determining the relative importance of surface and core states. In the smallest crystallites the number of surface Se orbitals is similar to the number of core Se orbitals making up the delocalized core state. The optical properties of the smallest dots are then strongly influenced by the surface, and are highly temperature dependent. With increasing size the surface component becomes less important. This is reflected in the decreasing temperature dependence of the shape of the FLN spectra. In fact, for 83-Å-diameter crystallites, both exciton–LO-phonon couplings ($S \sim 1.1$) and emission lifetimes ($\tau_r \sim 50$ nsec) remain virtually unchanged between 1.75 and 10 K. The absorbing and emitting states in these relatively large crystallites are well-defined core states with the surface acting as a small perturbation.

IV. FINAL REMARKS

This study describes the temperature and size dependence of exciton–LO-phonon couplings and emission lifetimes in nanometer-size CdSe crystallites (quantum dots). We find that in the smaller crystallites there is a dramatic increase in both the lifetime and the coupling to LO phonons as the temperature is decreased from 10 to

1.75 K. The Stokes shift is observed to increase with decreasing temperature, and both the linewidth and Stokes shift decrease with increasing crystallite diameter.

The temperature dependence of the luminescence observed here is similar to that observed in a wide range of random ternary II-VI alloys such as $CdS_{1-x}Se_x$ mixed crystals. In these bulk materials, disorder in the solid solutions leads to compositional fluctuations within the lattice, and localization of the exciton through localization of the hole. We suggest that in CdSe crystallites surface disorder yields random fluctuations in the hole electronic potential. The large exciton–LO-phonon couplings and microsecond lifetimes at the lowest temperatures and for the smaller crystallites result from the hole trapping or localizing on the surface. Phonon-assisted tunneling between localized states explains the decrease in the phonon coupling, the decrease in the Stokes shifts, and the decrease in the lifetimes as the temperature is increased. It must be stressed here that these surface fluctuations are extremely shallow (< 10 meV), and that the luminescence is "band edge" and not the deep red and mostly uncharacterized luminescence often observed in these materials.

The temperature dependence of the radiative lifetimes observed in this study is similar to that observed in nanocrystallites of Si[22] (Ref. 22) and in porous Si.[28] Spin dynamics have been used to explain the data in the Si systems.[28] Surface treatments of both nanocrystallites of Si and of porous Si are known to strongly affect luminescence quantum yields.[22,29] We speculate here that the surface localization model of this paper may also be applicable to some extent in the Si systems. We also cannot at this stage completely rule out spin dynamics as a contributing factor in explaining our data.

Semiconductor nanocrystallites have an unusually large surface-to-volume ratio. As a result, their electronic properties appear to be strongly influenced by the interface between the crystallites and the matrix in which they are embedded. The interfacial electronic states can in principle be exploited in the design of composite materials with enhanced optical/electronic properties. It should be possible to chemically modify this interface and thus alter the interaction of crystallites with their surroundings. The temperature dependence of exciton–LO-phonon couplings and the lifetime of the "band edge" luminescence may serve as valuable probes in determining the energetics of the interface.

ACKNOWLEDGMENTS

M.N., C.B.M., and M.G.B. benefited from support from AT&T, NSERC, and the Lucille and David Packard foundation, respectively. This work was funded in part by the MIT Center for Materials Science and Engineering (NSF-DMR-90-22933) and NSF (DMR-91-57491). We also thank the MIT Harrison Spectroscopy Laboratory (NSF-CHE-89-14953) for use of its facilities.

[1]Recent reviews include L. E. Brus, Appl. Phys. A **53**, 465 (1991); Y. Wang and N. Herron, J. Phys. Chem. **95**, 525 (1991); H. Weller, Angew. Chem. Int. Ed. Engl. **32**, 41 (1993).

[2]C. B. Murray, D. J. Norris, and M. G. Bawendi, J. Am. Chem. Soc. **115**, 8706 (1993).

[3]M. G. Bawendi, P. J. Carroll, W. L. Wilson, and L. E. Brus, J. Chem. Phys. **96**, 946 (1992).

[4]M. O'Neil, J. Marohn, and G. MacLendon, J. Phys. Chem. **89**, 3435 (1990).

[5]J. A. Eychmuller, A. Hasselbrath, L. Katsikas, and H. Weller, Ber. Bunsenges Phys. Chem. **95**, 79 (1991).

[6]S. Permogorov, A. Reznitski, S. Verbin, G. O. Muller, P. Flogel, and M. Nikiforova, Phys. Status Solidi B **113**, 589 (1982).

[7]S. Permogorov, A. Reznitski, V. Travnikov, S. Verbin, G. O. Muller, and M. Nikiforova, J. Lumin. **24/25**, 409 (1981).

[8]L. Becerra, C. B. Murray, R. G. Griffin, and M. G. Bawendi, J. Chem. Phys. **100**, 3297 (1994).

[9]A. P. Alivisatos, A. L. Harris, M. L. Steigerwald, and L. E. Brus, J. Chem. Phys. **89**, 7 (1988).

[10]M. G. Bawendi, W. L. Wilson, L. Rothberg, P. G. Carroll, T. M. Jedju, M. L. Steigerwald, and L. E. Brus, Phys. Rev. Lett. **65**, 1623 (1990).

[11]N. Peyghambarian, B. Fluegel, D. Hulin, A. Migus, M. Joffre, A. Antonetti, S. W. Koch, and M. Lindberg, IEEE J. Quantum Electron. **QE-25**, 2516 (1989).

[12]D. J. Norris, M. Nirmal, C. B. Murray, A. Sacra, and M. G. Bawendi, Z. Phys. D **26**, 355 (1993).

[13]J. J. Shiang, A. N. Goldstein, and A. P. Alivisatos, J. Chem. Phys. **92**, 3232 (1990); J. J. Shiang, S. H. Risbud, and A. P. Alivisatos, *ibid.* **98**, 8432 (1993).

[14]A. P. Alivisatos, T. D. Harris, P. J. Carroll, M. L. Steigerwald, and L. E. Brus, J. Chem. Phys. **90**, 3463 (1989).

[15]M. C. Klein, F. Hache, D. Ricard, and C. Flytzanis, Phys. Rev. B **42**, 11 123 (1990).

[16]S. Nomura and T. Kobayashi, Phys. Rev. B **45**, 1305 (1992).

[17]J. J. Hopfield, J. Phys. Chem. Solids **10**, 110 (1959).

[18]K. J. Nash, M. S. Skolnick, P. A. Claxton, and J. S. Roberts, Phys. Rev. B **39**, 5558 (1989).

[19]Y. R. Wang and C. B. Duke, Phys. Rev. B **37**, 6417 (1988).

[20]N. F. Mott and E. A. Davis, *Electronic Processes in Non-Crystalline Materials* (Clarendon, Oxford, 1971).

[21]T. Holstein, S. K. Lyo, and R. Orbach, in *Laser Spectroscopy*, edited by W. M. Yen (Spinger-Verlag, Berlin, 1981), p. 39.

[22]W. L. Wilson, P. F. Szajowski, and L. E. Brus, Science **262**, 1242 (1993).

[23]D. J. Norris, A. Sacra, C. B. Murray, and M. G. Bawendi, Phys. Rev. Lett. **72**, 2612 (1994).

[24]C. Gourdon and P. Lavallard, Phys. Status Solidi B **153**, 641 (1989).

[25]D. Ouadjaout and Y. Marfaing, Phys. Rev. B **46**, 7908 (1992).

[26]A. I. Ekimov, F. Hache, M. C. Schanne-Klein, D. Ricard, C. Flytzanis, I. A. Kudryavtsev, T. V. Yazeva, A. V. Rodina, and Al. L. Efros, J. Opt. Soc. Am. B **10**, 100 (1993).

[27]A. I. Ekimov, Al. L. Efros, M. G. Ivanov, A. A. Onushcenko, and S. K. Shumilov, Solid State Commun. **72**, 645 (1989).

[28]P. D. J. Calcott, K. J. Nash, L. T. Canham, M. J. Kane, and D. Brumhead, J. Phys. Condens. Matter **5**, L91 (1993).

[29]J. K. M. Chun, A. B. Bocarsly, T. R. Cottrell, J. B. Benzinger, and J. C. Yee, J. Am. Chem. Soc. **115**, 3024 (1993).